

Chromogenic Meroterpenoids from the Mushrooms *Russula ochroleuca* and *R. viscida*

Bernd Sontag,^{[a],[‡]} Matthias R uth,^{[a],[‡],[‡]} Peter Spitteller,^[a] Norbert Arnold,^[a] Wolfgang Steglich,^{*[a]} Matthias Reichert,^[b] and Gerhard Bringmann^{*[b]}

Dedicated to Professor Dieter Enders on the occasion of his 60th birthday

Keywords: Natural products / Meroterpenoids / Mushrooms / Rearrangements / Colour reaction

The spirodioxolactone ochroleucin A₁ (**1**) is responsible for the red colour produced when the stalk base of *Russula ochroleuca* and *R. viscida* is treated with aqueous KOH. The labile chromogen rearranges easily into the isomeric dilactone ochroleucin A₂ (**2**). Ochroleucin A₁ is accompanied by the biosynthetically related hemiacetal ochroleucin B (**5**). The new compounds, whose structures were established by MS and NMR methods, appear to be derived biosynthetically by

oxidative condensation of two monomeric units. One of them, 2,5-dihydroxy-4-(3-methylbut-3-en-1-ynyl)benzaldehyde (**6**), was detected in the crude toadstool extract by GC/MS comparison with a synthetic sample. The absolute configurations of the ochroleucins A₁ and B have been determined by quantum chemical calculation of their CD spectra. (  Wiley-VCH Verlag GmbH & Co. KGaA, 69451 Weinheim, Germany, 2006)

Introduction

Russula ochroleuca (Pers.) Fr. (German: Ockert ubling) is a medium-sized agaric with ochre to yellow cap, whitish gills and a white stem. The base of the stem is covered with ochraceous fibers, which can be interpreted as rest of the velum universale. This very common mushroom grows on sour soil in coniferous and deciduous forests and is in some regions the most abundant *Russula* species. It can be identified by a colour reaction, first reported by the Italian mycologist Galli:^[1] If a drop of aqueous KOH solution is applied to the yellowish base of the toadstool, an intense red spot is immediately formed, which changes to brown within a few minutes. This behaviour is only known from *R. ochroleuca*, *R. viscida*, *R. messapica*, and *R. insignis*.^[1] In this publication, we report on the isolation, structural elucidation and biosynthetic formation of the chromogenic principle from the first two species.

[a] Department Chemie der Ludwig-Maximilians-Universit t, Butenandtstr. 5–13, 81377 M nchen, Germany
Fax: +49-89-21807756
E-mail: wos@cup.uni-muenchen.de

[b] Institut f r Organische Chemie, Universit t W rzburg, Am Hubland, 97074 W rzburg, Germany
Fax: +49-931-8885323

E-mail: bringman@chemie.uni-wuerzburg.de
[‡] Present address: Discovery Partners International GmbH, Waldhofer Str. 104, 69123 Heidelberg, Germany

[‡‡] Present address: Roche Diagnostics GmbH, Medicinal Chemistry, Nonnenwald 2, Building 231/380, 82372 Penzberg, Germany
Supporting information for this article is available on the WWW under <http://www.eurjoc.org> or from the author.

Results and Discussion

Isolation of the Metabolites

To reveal the chemical structure of the chromogen, about 12 kg of fresh fruit bodies of *R. ochroleuca* were collected in spruce forests around Munich. Only the lower third of the stipes was extracted with EtOAc, resulting in a yellow solution which still displayed the red colour reaction after the addition of base. After removal of the solvent, the residue was fractionated by flash chromatography on silica gel. Fractions showing the colour reaction were combined and further purified by preparative HPLC on reversed phase. Two structurally related yellow pigments were isolated, which were named ochroleucins A₁ (**1**) and B (**5**). The latter is chemically stable and shows no discolouration with KOH, whereas ochroleucin A₁ is responsible for the red colour reaction. From 4 kg of fresh stipes, 18 mg of ochroleucin A₁ (**1**) and 36 mg of ochroleucin B (**5**) were obtained. Chromogen **1** is very labile and rearranges rapidly into a stable red isomer, ochroleucin A₂ (**2**). As a result of this rearrangement the purification of **1** by HPLC was difficult. Fractions containing pure **1** change their colour within a few minutes at room temperature from yellow to red and have therefore to be cooled to –78  C immediately.

Ochroleucins A₁ and A₂

Due to the instability of ochroleucin A₁ (**1**), no molecular ion peak could be detected by any of the available ioni-

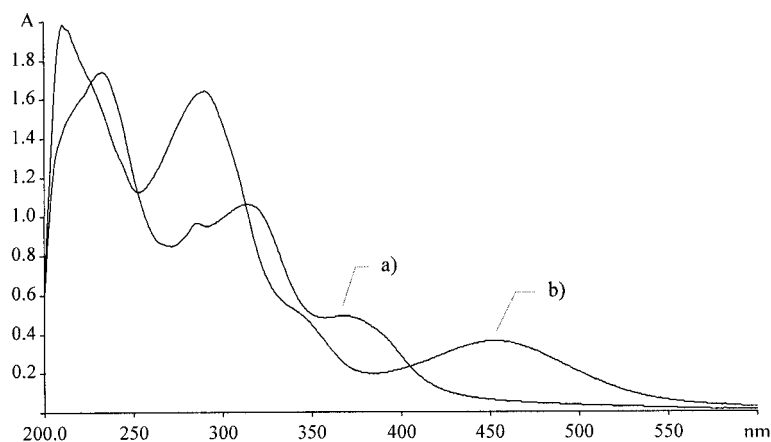


Figure 1. UV/Vis spectra of ochroleucin A₁ (**1**) in (a) MeOH and (b) MeOH + KOH.

sation modes (EI, FAB, ESI, APCI). Instead, the molecular composition of **1**, C₂₃H₁₄O₆, was derived indirectly from the highly resolved molecular ion $m/z = 386.0790$ of the stable isomer **2**. The UV/Vis spectrum of ochroleucin A₁ (**1**) in MeOH shows three main maxima at $\lambda_{\text{max}} = 233, 314,$ and 369 nm. On addition of base, the latter is shifted to 452 nm, thus explaining the red colour reaction (Figure 1). In the IR spectrum (KBr) a characteristic band of medium intensity at 2198 cm^{-1} indicates the presence of a doubly substituted triple bond. The surprisingly simple ¹H NMR spectrum of **1** shows two singlets at $\delta_{\text{H}} = 7.07$ and 7.58 ppm in the aromatic region, an additional singlet at $\delta_{\text{H}} = 9.65$ ppm for an aldehyde proton, and four doublets of quadruplets at $\delta_{\text{H}} = 5.47/5.56$ and $5.63/5.71$ ppm, revealing two olefinic methylene groups, connected by allylic coupling ($^4J = 0.6$ Hz) with methyl groups at $\delta_{\text{H}} = 2.01$ and 2.04 ppm, respectively. In addition, a broad signal at $\delta_{\text{H}} \approx 9.4$ ppm can be assigned to a phenolic OH group.

The ¹³C NMR spectrum of **1** exhibits signals for 23 carbon atoms in agreement with the molecular formula C₂₃H₁₄O₆. According to the DEPT spectrum, two methyl, two methylene, three methine, and 16 quaternary carbon atoms are present. COSY and HMBC experiments indicate that the methyl and methylene groups form part of two 3-methylbut-3-en-1-ynyl residues, in agreement with the signals in the ¹H NMR spectrum. The aromatic proton signal at $\delta_{\text{H}} = 7.07$ ppm shows HMBC correlations with four carbon atoms of a benzene ring, an aldehyde carbon atom ($\delta_{\text{C}} = 9.65$ ppm), and the α -alkynyl carbon atom of one of the side chains. From this information and chemical shift considerations, the partial structure A of a 2,5-dioxygenated

benzaldehyde can be proposed (Figure 2). In a similar fashion the HMBC correlations originating from the proton signal at $\delta_{\text{H}} = 7.58$ ppm reveal a cyclopentenedione unit B carrying the second methylbutenynyl residue. Connection of the two units A and B with the so far unconsidered CO group (signal at $\delta_{\text{C}} = 166.1$ ppm) leads to spiro lactone structure **1** for ochroleucin A₁ (Figure 3), in agreement with the IR absorption at 1809 cm^{-1} . The structure is supported by comparison of the NMR spectroscopic data of ochroleucin A₁ with those of simple cyclopent-4-ene-1,3-diones^[2] and the mutadiones, structurally related spirodioxolactones from the polypore *Hapalopilus mutans*.^[3]

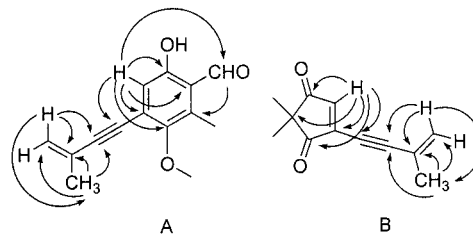


Figure 2. Partial structures A and B for ochroleucin A₁ (**1**) derived from HMBC experiments.

To determine the absolute configuration of ochroleucin A₁, quantum chemical circular dichroism (CD) calculations^[4,5] were performed. Arbitrarily starting with the (*R*) enantiomer of **1**, a conformational analysis on the semiempirical PM3^[6] level was carried out, resulting in five minimum structures within the energetically relevant range of $3\text{ kcal/mol}^{[7]}$ above the global minimum. For each of these geometries a single CD spectrum was computed by means

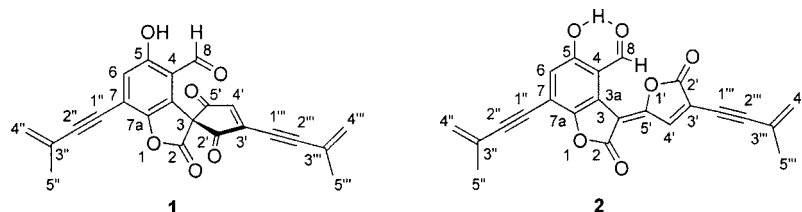


Figure 3. Structures of ochroleucin A₁ (**1**) and ochroleucin A₂ (**2**).

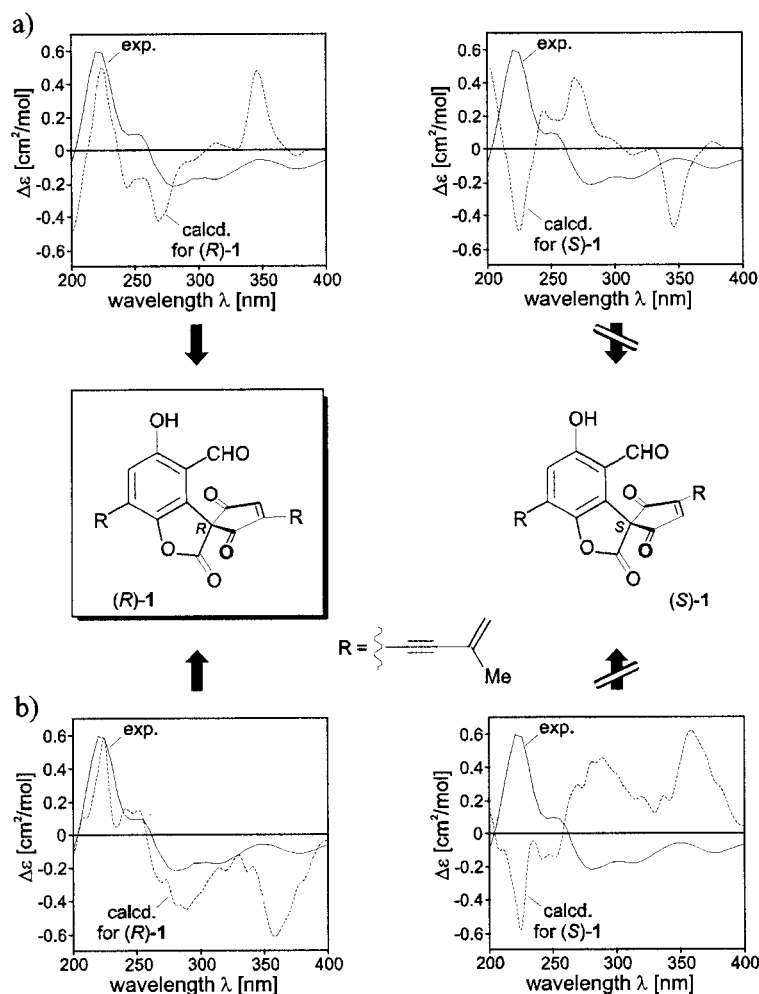


Figure 4. Attribution of the absolute configuration to ochroleucin A₁ (**1**) by CNDO/S-CI-CD calculations based on a) a conformational analysis and b) an MD simulation.

of the CNDO/S^[8] Hamiltonian. The resulting CD curves were summed up weighted, following the Boltzmann statistics, i.e., according to the heat of formation of the respective conformer. The overall CD spectrum thus obtained was subsequently UV-corrected^[9] and compared with the experimental one of ochroleucin A₁ (**1**), revealing a fairly good agreement with the simulated CD curve of (*R*)-**1** (Figure 4a, left) and a nearly mirror-image behaviour as compared to the one calculated for (*S*)-**1** (Figure 4a, right).

In order to confirm this result, additional CD calculations were performed for (*R*)-**1**, this time based on a molecular dynamics (MD) simulation using the TRIPOS^[10] force field at a virtual temperature of 500 K and a simulation length of 500 ps. For the geometries extracted every 0.5 ps from the trajectory of motion, single CD spectra were computed using again the CNDO/S-CI^[8] method. Summation of the resulting 1000 calculated CD curves and subsequent UV correction^[9] delivered the overall simulated CD spectrum, which again matched well with the measured one of **1** (Figure 4b, left), while the curve predicted for (*S*)-**1** was once again found to be virtually opposite (Figure 4b, right). Consequently, both theoretical approaches unambigu-

ously determined the absolute configuration of ochroleucin A₁ (**1**) as (*R*) (Figure 3).

The rearrangement of ochroleucin A₁ (**1**) into ochroleucin A₂ (**2**) occurs even in the solid state at $-20\text{ }^{\circ}\text{C}$ under argon. The less polar, deeply red ochroleucin A₂ (**2**) can be easily separated from unchanged **1** by preparative HPLC. Ochroleucin A₂ (**2**) exhibits a molecular ion peak at $m/z = 386$ in the high-resolution EIMS, corresponding to the molecular formula C₂₃H₁₄O₆. The ¹H NMR spectrum resembles that of ochroleucin A₁ (**1**); however, the signals in the aromatic region exhibit a low-field shift, most pronounced for the aldehyde proton, shifting from $\delta_{\text{H}} = 9.65$ to 10.80 ppm, and for the olefinic proton, shifting from $\delta_{\text{H}} = 7.58$ to 8.73 ppm. The phenolic proton, in the case of **1** occurring as a broad signal at $\delta_{\text{H}} \approx 9.4$ ppm, now appears as a sharp singlet at $\delta_{\text{H}} = 12.24$ ppm, indicating the formation of a strong hydrogen bond.^[11] Considering the HMBC correlations in the benzene part of the molecule, the partial structure A' can be proposed for ochroleucin A₂ (**2**, Figure 5). More severe changes are discernible in the cyclopentenone part of ochroleucin A₁ (**1**). The signals of the spirocarbon atom at $\delta_{\text{C}} = 66.4$ ppm and of the two carbonyl

groups are missing, and three new signals for quaternary C atoms at $\delta_C = 105.1$, 155.8, and 163.0 ppm are visible instead. From HMBC experiments and selective decouplings in the ^1H -coupled ^{13}C NMR spectrum, partial structure B' can be proposed (Figure 5). An alternative structure with the side chain at C-4 of the 2(5*H*)-furanone ring is excluded by the large $^3J_{\text{H,C}}$ coupling of 13 Hz between the ring proton and the lactone carbonyl group. Based on partial structures A' and B' and the remaining atoms as formulated in C' (Figure 5), the dilactone structure **2** can be assigned to ochroleucin A₂ (Figure 3).

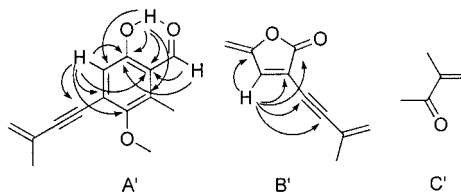


Figure 5. Partial structures A', B', and C' for ochroleucin A₂ (**2**) derived from HMBC experiments.

The rearrangement of **1** into **2** can be explained by opening of the spirodione ring at C-2' through traces of water and recyclization of the resulting enol carboxylic acid **3** into the thermodynamically more stable dilactone **2** (Figure 6). Interestingly, only the sterically less hindered of the two possible regioisomers of **2** is formed. Possibly, hydrolytic cleavage at C-5' also takes place; however, in this case recyclization of the enol carboxylic acid to the lactone is prohibited because of the strong steric interaction of the methylbutenynyl substituent with the coplanar carbonyl group of the neighbouring furanone ring. This regioselectivity agrees with the observation that the rearrangement of **1** into **2** proceeds only with low yield. Formation of an anion from **3** would lead to the highly delocalized species **4**, explaining the red colour reaction of ochroleucin A₁ (**1**) with base.

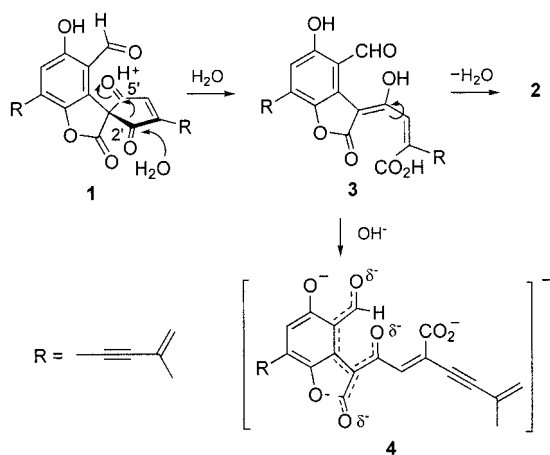


Figure 6. Rearrangement of ochroleucin A₁ (**1**) into ochroleucin A₂ (**2**) and formation of the red anion **4**.

Structurally, ochroleucin A₂ (**2**) resembles other fungal dilactones like variegatorubin,^[12] gomphilactone,^[13] and bovilactone-4,4.^[14] All of these metabolites are red pigments and exhibit similar NMR spectroscopic data for the

dilactone moiety, supporting the (*E*) configuration given for ochroleucin A₂ in structure **2**. This was confirmed by DFT calculations using the B3LYP^[15] hybrid functional with a 6-31G* basis set, favouring the (*E*) diastereomer over (*Z*) by 7.9 kcal/mol. This result can be explained by the mutual hydrogen bond formation in (*E*)-**2** between the hydrogen atom at the aldehyde functionality and the lactone oxygen atom at position 1', and between 4'-H and the carbonyl oxygen atom at C-2, leading to a planar minimum geometry of ochroleucin A₂ (**2**). By contrast, (*Z*)-**2** suffers from a steric hindrance between the aldehyde hydrogen atom and 4'-H, and from an electronical interference between O-1' and 2-O, resulting in a twisted minimum structure, and therefore in a significantly higher heat of formation.

Ochroleucin A₁ (**1**) is also responsible for the red colour reaction of *Russula viscida* Kudřna (German name: Lederstiel-Täubling) on treatment with aqueous base. In this case, small amounts of ochroleucin A₂ (**2**), but no ochroleucin B were detected. Preliminary experiments indicate that the chromogens of *R. insignis* Qu el. differ from those of the two other species.

Ochroleucin B

The second metabolite, ochroleucin B (**5**), shows a molecular ion peak at $m/z = 390$ in the high-resolution EIMS corresponding to the molecular formula C₂₄H₂₂O₅. In the NMR spectra, again signals for two 3-methylbut-3-en-1-ynyl residues can be identified. The ^1H NMR spectrum of ochroleucin B (**5**) resembles that of **1**; however, it lacks the signals for the aldehyde and phenolic protons. In addition two singlets at $\delta_{\text{H}} = 6.80$ and 6.45 ppm ($\delta_{\text{C}} = 113.2$ and 135.5 ppm), two methoxy signals at $\delta_{\text{H}} = 3.48/4.10$ ppm, and an AB quadruplet for a diastereotopic OCH₂ group ($\delta_{\text{H}} = 4.43/4.92$ ppm, $^2J = 16$ Hz; $\delta_{\text{C}} = 59.2$ ppm) can be recognized. Furthermore, two singlets at $\delta_{\text{H}} = 4.02$ ($\delta_{\text{C}} = 49.5$ ppm) and 3.21 ppm can be attributed to an aliphatic methine proton, and a tertiary OH group, respectively. In the ^{13}C NMR spectrum 24 signals can be identified, which, according to the DEPT spectrum, belong to four methyl, three methylene, and three methine groups and 14 quaternary carbon atoms. Only one carbonyl signal is visible at $\delta_{\text{C}} = 198.7$ ppm. From HMBC measurements and selective decouplings in the ^1H -coupled ^{13}C NMR spectrum (Figure 7), gross structure **5** can be assigned to ochroleucin B. Of special diagnostic value are the HMBC correlations of the methylene protons at C-5 as well as those of the angular proton 9b-H, which indicate a connection of the benzene ring with the cyclopentenone unit.

For a completion of the structural elucidation of **5**, the absolute configuration at the stereogenic centers C-3a and C-9b had to be determined. For this reason, quantum chemical CD calculations were performed, as in the case of ochroleucin A₁ (**1**). Due to the possible existence of four stereoisomers, two independent conformational analyses, one for the (3*aS*,9*bS*) and one for the (3*aS*,9*bR*) diastereomer of **5**, were launched using the semiempirical

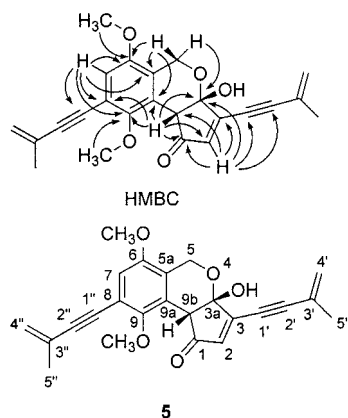


Figure 7. Selected HMBC correlations and structure of ochroleucin B (**5**).

PM3^[6] method, resulting in 50 and 41 minimum geometries, respectively.^[7]

These structures were submitted to CD calculations, as described above, this time only by means of the OM2^[16] instead of the CNDO/S^[8] Hamiltonian. The comparisons of the four UV-corrected^[9] overall CD spectra thus obtained with the measured curve are displayed in Figure 8:

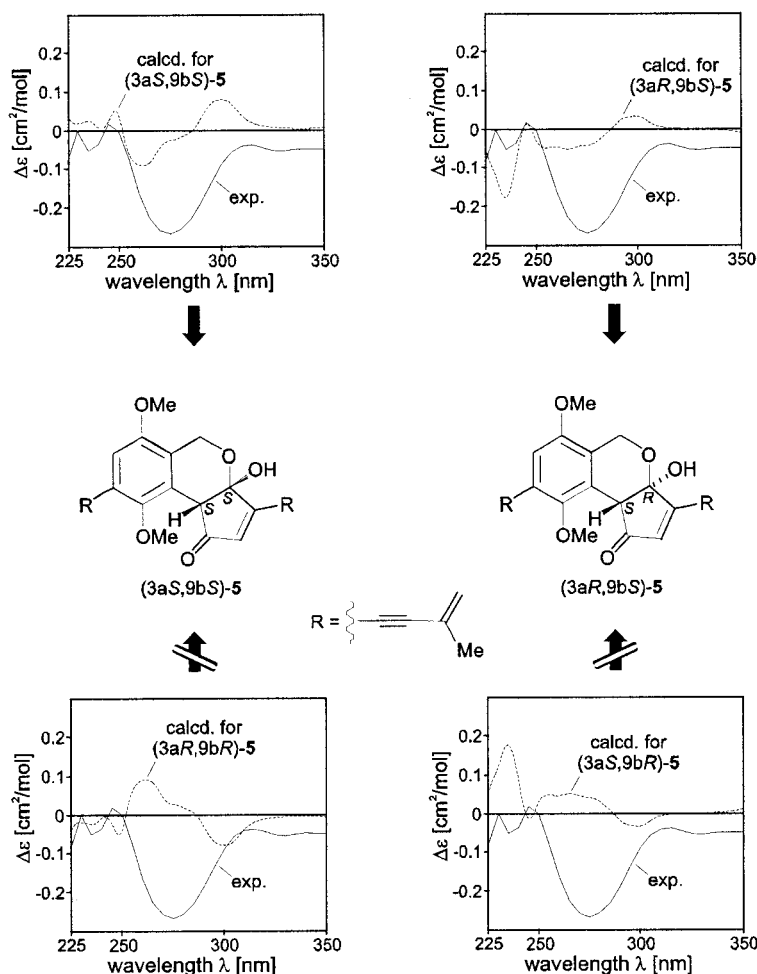


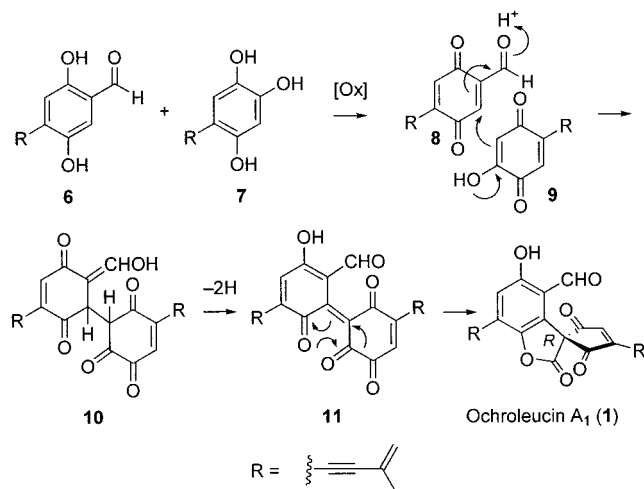
Figure 8. Comparison of the OM2-predicted CD spectra for the four possible diastereomers of ochroleucin B (**5**) with the experimental CD curve.

While the theoretical spectra for both, the (3a*S*,9b*S*) and the (3a*R*,9b*S*) diastereomers, match the experiment quite well (Figure 8, top), the CD curves for (3a*S*,9b*R*)-**5** and (3a*R*,9b*R*)-**5** both behave almost oppositely as compared to the experimental one (Figure 8, bottom). Therefore, only the stereogenic centre at C-9b can unambiguously be assigned as (*S*) by the calculations. From thermodynamic considerations, however, one should expect C-3a to be (*S*)-configured, too, since the (*S,S*) diastereomer of **5**, with its relative *cis* configuration, is drastically favoured over the *trans* isomer, by 16.7 kcal/mol, according to the PM3 calculations. This assignment is confirmed by considerations on the biosynthetic formation of **5** (see below).

Biosynthetic Considerations

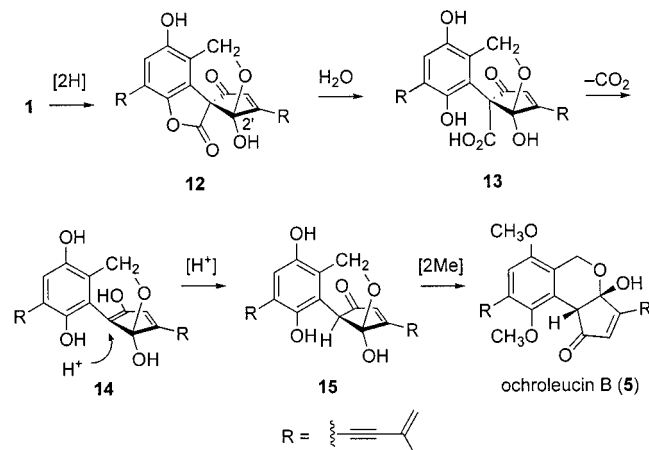
The structures of the ochroleucins and their co-occurrence suggest a close biogenetic relationship. Ochroleucin A₁ (**1**) could be formed by oxidative coupling of two monomeric precursors **6** and **7**. After conversion into the corresponding benzoquinones **8** and **9**, they might undergo a Michael addition to form the dimer **10**, which should then be oxidized to the tetraketone **11**. Rearrangement of this

intermediate as indicated by the arrows would afford ochroleucin A₁ (**1**).^[17] Since only the (3*R*) isomer is formed, the stereochemistry of the rearrangement appears to be controlled by an enzyme (Scheme 1).



Scheme 1. Proposal for the biosynthesis of ochroleucin A₁ (**1**).

The further pathway from **1** to ochroleucin B (**5**) involves reduction of the aldehyde group followed by regioselective attack of the resulting carbinol at the 2'-carbonyl group to yield the cyclic hemiacetal **12** with (2'*S*) configuration. Hydrolytic opening of the lactone ring would afford the β -oxo acid **13**, and, after decarboxylation, enol **14**. Protonation of **14** from the *Re* face, followed by dimethylation of the resulting diphenol **15**, would lead to ochroleucin B (**5**) with the more favourable *cis* configuration. While the (*S*) configuration at C-3a of **5** is directly determined by the mechanistic considerations displayed in Scheme 2, leading to the correct constitution of ochroleucin B (**5**) as deduced by NMR experiments (see above), the absolute configuration at C-9b can mechanistically not be assigned a priori, since the protonation of **14** could, in principle, take place from both sides. But in combination with the results of the CD calculations (see above), which unambiguously deter-



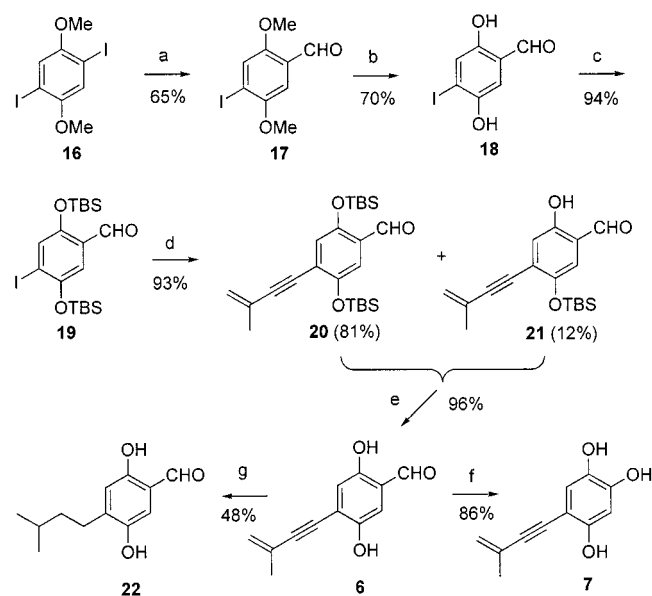
Scheme 2. Mechanistic proposal for the biosynthetic formation of ochroleucin B (**5**) from ochroleucin A₁ (**1**).

mine the stereogenic center at C-9b as (*S*), the absolute configuration of ochroleucin B (**5**) can now clearly be assigned as (3*aS*,9*bS*).

Meroterpenoids with 3-methylbut-3-en-1-yl side chains similar to the potential precursors **6** and **7** are known as fungal metabolites, e.g., eutypine, a plant pathogen from *Eutypa lata*,^[20] siccayne from *Helminthosporium siccans*,^[21] asperptyne from *Aspergillus duricaulis*,^[22] and sterehirsutinal from *Stereum hirsutum*.^[23]

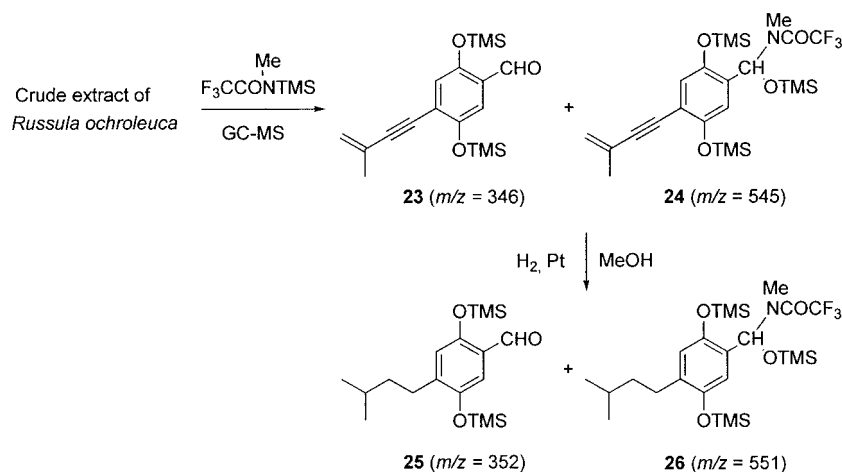
Synthesis of the Presumed Ochroleucin Precursors

In order to obtain experimental evidence for the proposed biosynthesis, the suggested precursors **6** and **7** were synthesized (Scheme 3). The synthesis of **6** starts from 1,4-diiodo-3,5-dimethoxybenzene (**16**),^[24] which was efficiently transformed into the iodo aldehyde **17** according to a known procedure.^[25] Demethylation of **17** with BBr₃ gave the dihydroxy aldehyde **18**, which was converted into the bis(*tert*-butyldimethylsilyl) (TBS) derivative **19**. Sonogashira coupling of **19** with 3-methylbut-3-en-1-yne^[26] afforded the alkenynyl derivative **20** and small quantities of the monodesilylated product **21** in excellent yields. Desilylation of this mixture with *n*-tetrabutylammonium fluoride in acetic acid provided the desired monomer **6**, which could be converted into the trihydroxy compound **7** by Dakin reaction with sodium percarbonate. Catalytic hydrogenation of precursor **6** yielded the perhydro derivative **22**. The overall yields of compounds **6**, **7**, and **22** were 38, 32, and 18%, respectively.



Scheme 3. Synthesis of the monomeric precursors **6** and **7**; reagents and conditions: a) *n*BuLi, Et₂O, then DMF; b) BBr₃; c) TBSCl, imidazole, DMAP; d) 3-methylbut-3-en-1-yne, cat. Pd(PPh₃)₂Cl₂, CuI, THF; e) *n*Bu₄NF, AcOH; f) Na₂CO₃ × 1.5 H₂O₂, THF; g) H₂, PtO₂.

With the potential precursors **6** and **7** at hand, experiments were performed to detect these compounds in the



Scheme 4. Detection of the monomeric precursor **6** in the crude extract of *R. ochroleuca* by GC/MS.

mushroom extract. Accordingly, fresh stipes of *R. ochroleuca* were treated with MeOH, and the extract was prepurified by preparative HPLC on RP-18. Fractions with the same retention times as synthetic **6** and **7** were collected separately, per(trimethylsilyl)ated with *N*-methyl-*N*-(trimethylsilyl)trifluoroacetamide (MSTFA), and subjected to GC/MS analysis. The aldehyde **6** was thus identified as the expected bis(trimethylsilyl) derivative **23** and its MSTFA adduct **24** (Scheme 4). Both derivatives appeared at the same retention times and showed the same characteristic mass spectrometric fragmentation patterns as the silylation products derived from synthetic aldehyde **6**. This result was confirmed by catalytic hydrogenation of the crude fungal extract, followed by trimethylsilylation with MSTFA and subsequent GC/MS analysis. By comparison with an authentic sample of the hexahydro derivative **22**, subjected to the same procedure, the two silyl derivatives **25** and **26** could be identified unambiguously.

Attempts to identify the benzenetriol **7** by the same protocol failed, probably due to its instability. Even synthetic **7** could only be characterized after immediate transformation into the per(trimethylsilyl) derivative. The identification of the TMS derivatives of homogentisic acid, gentisic acid (trace), gentisaldehyde (trace), and gentisyl alcohol in the crude extract points to tyrosine as biosynthetic precursor of the ochroleucins.^[27]

Conclusion

In summary, the paper shows the interplay of biological observations, biosynthetic considerations, synthetic studies, and modern techniques of isolation and structural elucidation including efficient quantum chemical calculations. The ochroleucins **1** and **5** and their biogenetic precursor **6** represent the first meroterpenoids from a *Russula* species. Simple prenylated derivatives of benzene-1,4-diol are known from the related genus *Lactarius* (Russulaceae).^[28,29]

Experimental Section

General: Optical rotations: Perkin–Elmer 214. UV/Vis: Perkin–Elmer Lambda 16. IR: Perkin–Elmer FT-IR 1000. NMR: Bruker ARX-300, AMX-600 and Varian VXR-400 S, in CDCl₃ with the solvent peak as internal standard. Multiplets due to ¹J(C,H) couplings are indicated by capital letters. MS: Finnigan MAT 90 and MAT 95Q. Solid-phase extractions: Chromabond C18 cartridges (Macherey–Nagel). TLC: Merck, silica HPTLC plates Kieselgel 60 F₂₅₄ S, 0.2 mm, solvent system (v/v): EtOAc/hexanes, 1:2. Analytical HPLC: Waters 600 E Pump and System Controller with Photodiode Array Detector 990+. Knauer Vertex columns 4 × 250 mm, packing material Nucleosil 100 C18, 5 μm. Eluent A: H₂O/MeCN, 9:1; eluent B: MeCN. Linear gradient: 0 min: A 100%, 30 min: B 100%; flow rate 1 mL/min, detection range 200–400 nm. Preparative HPLC for the isolation of **1**, **2**, and **5**: Merck Hitachi L 6200 Intelligent Pump and 655A Variable Wavelength UV Monitor. Knauer Vertex column 16 × 250 mm, packing material Nucleosil 100 C18, 7 μm. Eluent A: H₂O/MeCN, 9:1; eluent B: MeCN. Gradient: 0 min: A 100%, B 30 min: 100%; flow rate: 7 mL/min, detection at 300 nm. Preparative HPLC for the identification of **6**: Pumps: Waters 590 EF. Injector: U6K. Detector: Knauer Variable Wavelength Monitor. Detection at 300 nm. Column: 16 × 250 mm, Nucleosil 100 C18, 7 μm (Knauer). Gradient: 0 min: 100% H₂O, 40 min: 100% MeOH; flow rate: 6 mL/min. GC/MS: Finnigan MAT 90 double focussing mass spectrometer, equipped with an EI ion source operating at 70 eV. For GC-MS a Varian GC 3400 gas chromatograph with a fused silica DB-5ms capillary column (30 m × 0.25 mm, coated with a 0.25 μm layer of liquid phase) and helium as carrier gas was used for sample separation. The injector temperature was kept at 300 °C, injection volumes were 0.2–0.4 μL of a 1–2% (m/v) solution. Temperature programme: 2 min isothermal at 50 °C, then 10 °C/min up to 300 °C, finally 10 min isothermal at 300 °C. Retention indices *R*_i were determined by co-injection of a 0.2 μL sample of a standard mixture of saturated straight-chain alkanes C₁₀–C₃₆.

Mushrooms: *R. ochroleuca* was collected in autumn 1996, 1997, and 1998 in spruce forests around München (leg./det. B. Sontag). Two fruit bodies of the rare *R. viscida* were collected in August 1998 under *Picea* near Herrsching, Bavaria (leg./det. N. Arnold).

Isolation Procedure: In a typical workup, 4 kg of the lower third of the frozen stipes (corresponding to 12 kg of fresh fungi) was ex-

tracted with EtOAc (5 × 3 L), until the resulting solution was colourless. After removal of the solvent, the strongly smelling, brown, oily residue (ca. 50 g) was dissolved in hexanes/EtOAc (2:1) and purified by chromatography on silica gel with the same solvent mixture. The first eluting yellow fraction contained ochroleucin B (2), the slower moving, weakly orange fraction mainly ochroleucin A₁ (1). After removal of the solvent under reduced pressure, each fraction was further purified by preparative HPLC on a reversed phase column [Nucleosil-100 C-18, 7 µm, 16 × 250 mm (Knauer); solvent A: H₂O/MeCN, 9:1; solvent B: MeCN; gradient: start 100% A, linear in 30 min to 100% B; flow rate: 7 mL/min] to afford ochroleucin B (5, 36 mg, 0.0003%) and ochroleucin A₁ (1, 18 mg, 0.00015%). In the case of *R. viscida*, the yellow stipes from two specimens (30 g) were extracted overnight with EtOAc (100 mL). Direct analysis of this extract by TLC and analytical HPLC revealed the presence of 1 and 2. Ochroleucin B (5) could not be detected.

Ochroleucin A₁ (1): Orange-yellow gum. *R_f* (TLC) = 0.44, orange-yellow spot, red with KOH. $[\alpha]_D^{29} = -200$ (*c* = 0.002, MeOH). UV (MeOH): λ_{\max} (log ϵ) = 233 (4.38), 314 (4.17), 369 (3.84) nm. UV (MeOH + 100 µl 4% KOH in MeOH): λ_{\max} (log ϵ) = 210 (4.44), 290 (4.36), 337 sh (3.88), 452 (3.71) nm. CD (MeOH): λ ($\Delta\epsilon$) = 221 (+0.64), 246 (+0.08), 251 (+0.10), 279 (−0.23), 297 (−0.17), 313 (−0.18), 349 (−0.06), 377 (−0.12) nm. IR (KBr): $\tilde{\nu}$ = 3432 (s, br), 2928 (m), 2198 (m), 1809 (m), 1716 (s), 1676 (w), 1619 (m), 1419 (m), 1284 (w), 1252 (w), 1216 (w), 990 (m) cm^{−1}. ¹H NMR (600 MHz, CDCl₃): δ = 2.01 (dd, *J* = 1.8, 0.6 Hz, 3 H, 5''-CH₃), 2.04 (dd, *J* = 1.8, 0.6 Hz, 3 H, 5'''-CH₃), 5.47 (m, 1 H, 4''-H), 5.56 (m, 1 H, 4'''-H), 5.63 (m, 1 H, 4''''-H), 5.71 (m, 1 H, 4''''-H), 7.07 (s, 1 H, 6-H), 7.58 (s, 1 H, 4'-H), 9.40 (br, 1 H, 5-OH), 9.65 (s, 1 H, 8-H) ppm. ¹³C NMR (150 MHz, CDCl₃): δ = 22.5 (C-5'''), 22.9 (C-5''), 66.4 (C-3), 77.7 (C-1'''), 80.3 (C-1''), 101.1 (C-2''), 114.9 (C-2'''), 116.4 (C-3a), 121.7 (C-7), 122.4 (C-6), 125.4 (C-4''), 125.5 (C-3'''), 125.8 (C-3''), 128.4 (C-4'''), 128.5 (C-4), 147.3 (C-4'), 147.4 (C-3'), 149.2 (C-7a), 157.7 (C-5), 166.1 (C-2), 188.7 (C-5'), 188.8 (C-8), 190.7 (C-2') ppm. MS: No [M⁺], [M + H]⁺ or [M − H][−] were observed in any ionisation mode.

Rearrangement of 1 into 2: A solution of 1 (12 mg) in MeCN (5 mL) was stirred at room temperature for 12 d and the resulting mixture of 1 and 2 was separated by preparative HPLC as described above. Yield: 2 mg of 2.

Ochroleucin A₂ (2): Red gum. *R_f* (TLC) = 0.89, red spot. UV (MeCN): λ_{\max} (log ϵ) = 201 (4.00), 300 (3.82), 311 sh (3.78), 402 (3.54), 489 (3.39) nm. IR (KBr): $\tilde{\nu}$ = 3435 (s, br), 2924 (s), 2852 (s), 2197 (w), 1782 (w), 1735 (w), 1654 (w), 1458 (w), 1382 (w), 1261 (w), 1178 (w), 912 (w) cm^{−1}. ¹H NMR (600 MHz, CDCl₃): δ = 2.02 (m, 6 H, 5''-CH₃ + 5'''-CH₃), 5.47 (m, 1 H, 4''-H), 5.56 (m, 1 H, 4'''-H), 5.57 (m, 1 H, 4''''-H), 5.68 (m, 1 H, 4''''-H), 7.15 (s, 1 H, 6-H), 8.73 (s, 1 H, 4'-H), 10.80 (s, 1 H, 8-H), 12.24 (s, 1 H, 5-OH) ppm. ¹³C NMR (150 MHz, CDCl₃): δ = 22.3 (Qdd, *J* = 130, 11, 4 Hz, C-5'''), 23.2 (Qdd, *J* = 130, 11, 4 Hz, C-5''), 78.5 (d, *J* = 4 Hz, C-1'''), 80.3 (d, *J* = 6 Hz, C-1''), 100.5 (m, C-2''), 105.1 (s, C-3), 108.1 (m, C-2'''), 113.1 (ddd, *J* = 21, 6, 6 Hz, C-4), 116.5 (d, *J* = 2 Hz, C-3a), 120.3 (s, C-7), 121.8 (d, *J* = 2 Hz, C-3'), 124.9 (Ddd, *J* = 167, 8, 2 Hz, C-6), 125.3 (Tq, *J* = 159, 6 Hz, C-4''), 125.6 (qdd, *J* = 7, 2, <1 Hz, C-3''), 125.9 (qdd, *J* = 7, 2, <1 Hz, C-3'''), 127.6 (Tq, *J* = 154, 6 Hz, C-4'''), 139.0 (D, *J* = 189 Hz, C-4'), 147.9 (d, *J* = 10 Hz, C-7a), 155.8 (d, *J* = 8 Hz, C-5'), 160.0 (ddd, *J* = 5, 5, 3 Hz, C-5), 163.0 (d, *J* = 13 Hz, C-2'), 165.8 (s, C-2), 196.6 (D, *J* = 186, C-8) ppm. EI MS (DI, 220 °C, 70 eV): *m/z* (%) = 386 (100) [M⁺], 358 (7) [M − CO]⁺, 330 (10) [M − 2 CO]⁺, 240 (14), 135 (14), 98 (26), 83 (20), 69 (26), 55 (26). C₂₃H₁₄O₆: calcd. 386.0790; found 386.0792 (HR EI-MS).

Ochroleucin B (5): Yellow gum. *R_f* (TLC) = 0.70, yellow spot, brown with KOH. $[\alpha]_D^{30} = -17$ (*c* = 0.33, CHCl₃). UV (CHCl₃): λ_{\max} (log ϵ) = 286 (3.07), 312 (2.92) nm. CD (MeCN): λ ($\Delta\epsilon$) = 230 (−0.004), 237 (−0.06), 251 (+0.10), 247 (+0.02), 275 (−0.27), 314 (−0.04) nm. IR (KBr): $\tilde{\nu}$ = 3434 (s, br), 2923 (m), 2194 (m), 1711 (s), 1615 (m), 1483 (w), 1460 (m), 1406 (m), 1232 (s), 1073 (m), 904 (w) cm^{−1}. ¹H NMR (600 MHz, CDCl₃): δ = 2.02 (dd, *J* = 1.8, 0.6 Hz, 3 H, 5''-CH₃), 2.03 (dd, *J* = 1.8, 0.6 Hz, 3 H, 5'-CH₃), 3.78 (s, 3 H, 6-OCH₃), 4.02 (s, 1 H, 9b-H), 4.10 (s, 3 H, 9-OCH₃), 4.43 (d, *J* = 16 Hz, 1 H, 5-H), 4.92 (d, *J* = 16 Hz, 1 H, 5-H), 5.32 (m, 1 H, 4''-H), 5.42 (m, 1 H, 4''-H), 5.52 (m, 1 H, 4'-H), 5.60 (mq, 1 H, 4'-H), 6.45 (s, 1 H, 2-H), 6.80 (s, 1 H, 7-H) ppm. ¹³C NMR (150 MHz, CDCl₃): δ = 22.9 (Qdd, *J* = 129, 11, 6 Hz, C-5'), 23.3 (Qdd, *J* = 129, 11, 6 Hz, C-5''), 49.5 (Dm, *J* = 134 Hz, C-9b), 55.7 (Q, *J* = 144 Hz, 6-OCH₃), 59.2 (Td, *J* = 149, 2 Hz, C-5), 62.0 (Q, *J* = 145 Hz, 9-OCH₃), 79.2 (d, *J* = 5 Hz, C-1'), 85.1 (d, *J* = 6 Hz, C-1''), 95.5 (m, C-2''), 101.1 (m, C-3a), 108.9 (m, C-2'), 113.2 (D, *J* = 162 Hz, C-7), 115.3 (d, *J* = 1 Hz, C-8), 121.9 (Tq, *J* = 159, 6 Hz, C-4''), 123.4 (m, C-9a), 124.1 (m, C-5a), 125.7 (qdd, *J* = 6, 2, <1 Hz, C-3'), 126.2 (Tq, *J* = 161, 6 Hz, C-4'), 126.9 (qdd, *J* = 6, 2, <1 Hz, C-3''), 135.5 (D, *J* = 177 Hz, C-2), 150.2 (m, C-6), 152.1 (s, C-3), 154.4 (m, C-9), 198.7 (dd, *J* = 7, 4 Hz, C-1) ppm. EI MS (DI, 220 °C, 70 eV): *m/z* (%) = 390 (100) [M]⁺, 362 (14), 347 (13), 317 (11), 315 (11), 151 (20), 149 (52), 135 (16), 121 (20), 109 (22), 107 (21), 95 (42), 91 (37), 81 (46), 69 (42), 57 (47), 55 (58). (+)-FAB-MS: *m/z* (%) = 391 (32) [M + H]⁺, 390 (29) [M]⁺. C₂₄H₂₂O₅: calcd. 390.1454; found 390.1453 (HR EIMS).

4-Iodo-2,5-dimethoxybenzaldehyde (17): To a suspension of 1,4-diiodo-2,5-dimethoxybenzene (16)^[23] (2.0 g, 5.13 mmol) in dry Et₂O (60 mL) was added dropwise at 0 °C a solution of *n*-BuLi (2.5 M in *n*-hexane, 2.05 mL, 5.13 mmol) in dry Et₂O (7 mL). To the resulting clear solution a mixture of DMF (0.6 mL, 7.69 mmol) and dry Et₂O (5 mL) was slowly added, and the stirring continued at room temperature for 3 h. Then, the slightly yellow suspension was quenched with water (200 mL). The organic phase was separated and the aqueous phase extracted with Et₂O (3 × 200 mL). The combined organic phases were washed with water (200 mL) and brine (200 mL), and dried (MgSO₄). Concentration under reduced pressure yielded yellow crystals, which were purified by flash chromatography (hexanes/EtOAc, 9:1) to yield 17 (0.98 g, 65%) as a colourless solid. M.p. 109 °C. *R_f* (TLC) = 0.42 (hexanes/EtOAc, 5:1). UV (MeOH): λ_{\max} (log ϵ) = 206 (4.18), 229 (4.05), 273 (3.90), 351 (3.70) nm. ¹H NMR (CDCl₃, 300 MHz): δ = 3.88, 3.90 (each s, 3 H, OMe), 7.23 (s, 1 H), 7.47 (s, 1 H), 10.40 (s, 1 H, CHO) ppm. ¹³C NMR (CDCl₃, 75.5 MHz): δ = 56.4, 56.9 (each CH₃), 95.9 (C_q), 108.0, 123.7 (each CH), 125.1, 152.8, 156.2 (each C_q), 189.0 (CHO) ppm. MS (EI): *m/z* (%) = 292 (100) [M⁺], 277 (27) [M − CHO]⁺, 246 (10). C₉H₉IO₃ (292.07): calcd. C 37.01, H 3.11; found C 36.77, H 3.00.

2,5-Dihydroxy-4-iodobenzaldehyde (18): To a solution of 17 (1.0 g, 3.42 mmol) in dry CH₂Cl₂ (50 mL) was slowly added at −78 °C a solution of BBr₃ (4.32 g, 17.1 mmol) in dry CH₂Cl₂ (10 mL). The cooling bath was removed and the reaction mixture stirred at room temperature for 12 h. Then, the mixture was quenched with ice-cold water (100 mL), and after phase separation, the aqueous phase was extracted with CH₂Cl₂ (3 × 100 mL). The combined organic phases were subsequently washed with water (100 mL) and brine (100 mL), and dried (MgSO₄). Concentration in vacuo and purification of the residue by flash chromatography on silica gel (hexanes/EtOAc, 3:2) yielded 18 (0.62 g, 70%) as a yellow solid. M.p. 102 °C. *R_f* (TLC) = 0.51 (hexanes/EtOAc, 3:2). UV (MeOH): λ_{\max} (log ϵ) = 211 (4.03), 234 (3.93), 278 (3.97), 365 (3.59) nm. ¹H NMR ([D₆]DMSO, 300 MHz): δ = 7.03, 7.47 (each s, 1 H), 9.99, 10.16,

10.17 (each s, 1 H) ppm. ^{13}C NMR ($[\text{D}_6]\text{DMSO}$, 75.5 MHz): $\delta = 96.1$ (C_q), 111.0 (CH), 123.0 (C_q), 127.4 (CH), 149.9, 153.8 (each C_q), 190.2 (CHO) ppm. MS (EI): m/z (%) = 264 (100) [M^+], 263 (31) [$\text{M} - \text{CH}_3$] $^+$, 246 (3), 236 (10), 218 (3). $\text{C}_7\text{H}_5\text{IO}_3 \cdot 0.5\text{H}_2\text{O}$ (264.02): calcd. C 30.79, H 2.22; found C 30.80, H 2.49.

2,5-Bis(*tert*-butyldimethylsilyloxy)-4-iodobenzaldehyde (19): 18 (2.0 g, 7.6 mmol), imidazole (2.1 g, 30.4 mmol), *tert*-butyldimethylsilyl chloride (2.9 g, 19 mmol), and a small quantity of DMAP were dissolved in anhydrous DMF (60 mL) and heated at 50 °C for 18 h. After cooling, the reaction mixture was poured into water (200 mL) and extracted with Et_2O (5×150 mL). The combined organic phases were washed with water (250 mL) and brine (250 mL), and dried (MgSO_4). After concentration in vacuo, the brownish residue was purified by flash chromatography on silica gel (hexanes/EtOAc, 10:1) to yield **19** (3.51 g, 94%) as a colourless solid. M.p. 84 °C. R_f (TLC) = 0.78 (hexanes/EtOAc, 10:1). ^1H NMR (CDCl_3 , 300 MHz): $\delta = 0.26, 0.28$ (each s, 6 H, 2 CH_3), 1.01, 1.05 (each s, 9 H, 3 CH_3), 7.16, 7.35 (each s, 1 H), 10.32 (s, 1 H, CHO) ppm. ^{13}C NMR (CDCl_3 , 75.5 MHz): $\delta = -4.4, -4.1$ (each 2 CH_3), 18.3 (2 C_q), 25.7, 25.9 (each 3 CH_3), 100.2 (C_q), 114.6 (CH), 127.5 (C_q), 131.3 (CH), 149.9, 152.6 (each C_q), 189.4 (CHO) ppm. MS (EI): m/z (%) = 477 (2) [$\text{M} - \text{CH}_3$] $^+$, 436 (26) [$\text{M} - \text{C}_4\text{H}_8$] $^+$, 435 (100) [$\text{M} - \text{C}_4\text{H}_9$] $^+$, 309 (11), 307 (7), 251 (11). $\text{C}_{19}\text{H}_{33}\text{IO}_3\text{Si}_2$ (492.54): calcd. C 46.33, H 6.75; found C 46.95, H 6.72.

2,5-Bis(*tert*-butyldimethylsilyloxy)-4-(3-methylbut-3-en-1-ynyl)benzaldehyde (20): To a solution of **19** (6.0 g, 12.2 mmol), 3-methylbut-3-en-1-yne (3.4 mL, 36.3 mmol), bis(triphenylphosphane)palladium dichloride (0.200 g, 0.28 mmol) and CuI (0.042 g, 0.22 mmol) in dry THF (200 mL) was added triethylamine (102 mL, 0.73 mmol). The mixture was refluxed for 12 h, whereby a colourless deposit formed. After cooling, the suspension was filtered through Celite and concentrated in vacuo. The resulting solid residue was dissolved in Et_2O (250 mL), washed with brine (3×200 mL), and dried (MgSO_4). Evaporation of the solvent under reduced pressure yielded an oily residue that was flash-chromatographed on silica gel (hexanes/EtOAc, 15:1) to yield **20** (4.22 g, 81%) and the 2-*O*-desilylated analogue **21** (0.47 g, 12%).

20: Yellowish solid. M.p. 75 °C. R_f (TLC) = 0.84 (hexanes/EtOAc, 15:1). UV (MeOH): λ_{max} (log ϵ) = 205 (4.45), 223 (sh, 4.41), 293 (4.28), 360 (4.00) nm. ^1H NMR (CDCl_3 , 300 MHz): $\delta = 0.24, 0.26$ (each s, 6 H, 2 CH_3), 1.01, 1.02 (each s, 9 H, 3 CH_3), 1.99 (dd, $^4J_{\text{H,H}} = 1.5, 1.1$ Hz, 3 H, 5'- CH_3), 5.35, 5.43 (each m, 1 H, 4'- CH_2), 6.87, 7.20 (each s, 1 H), 10.34 (s, 1 H, CHO) ppm. ^{13}C NMR (CDCl_3 , 75.5 MHz): $\delta = -4.4$ (4 CH_3), 18.2, 18.3 (each C_q), 23.3 (CH_3), 25.7 (6 CH_3), 85.0, 97.6 (each C_q), 117.0 (CH), 123.0 (=CH $_2$), 123.4 (C_q), 124.4 (CH), 126.7, 127.2, 150.6, 152.2 (each C_q), 189.3 (CHO) ppm. MS (EI): m/z (%) = 415 (2) [$\text{M} - \text{CH}_3$] $^+$, 373 (100) [$\text{M} - \text{C}_4\text{H}_9$] $^+$. $\text{C}_{24}\text{H}_{38}\text{O}_3\text{Si}_2 \cdot \text{H}_2\text{O}$ (430.23): calcd. C 64.24, H 8.98; found C 64.53, H 8.89.

21: Yellow oil. R_f (TLC) = 0.63 (hexanes/EtOAc, 15:1). ^1H NMR (CDCl_3 , 300 MHz): $\delta = 0.24$ (s, 6 H, 2 CH_3), 1.04 (s, 9 H, 3 CH_3), 1.99 ("s", 3 H, CH_3), 5.37, 5.44 (each "s", 1 H, =CH $_2$), 6.92, 7.00 (each s, 1 H), 9.78 (s, 1 H, OH), 10.55 (s, 1 H, CHO) ppm. ^{13}C NMR (CDCl_3 , 75.5 MHz): $\delta = -4.4$ (2 CH_3), 18.2 (C_q), 23.2 (CH_3), 25.7 (3 CH_3), 84.9, 98.3, 120.1 (each C_q), 121.8, 122.2 (CH), 123.4 (=CH $_2$), 125.6, 126.5, 148.8, 155.4 (each C_q), 195.4 (CHO) ppm. MS (EI) m/z (%) = 316 (7) [M^+], 261 (8), 260 (23), 259 (100) [$\text{M} - \text{C}_4\text{H}_9$] $^+$, 219 (11). HRMS (EI): $m/z = 316.1051$ [M^+] (calcd. for $\text{C}_{18}\text{H}_{24}\text{O}_3\text{Si}$: 316.1495). $\text{C}_{18}\text{H}_{24}\text{O}_3\text{Si} \cdot 0.5\text{H}_2\text{O}$ (316.47): calcd. C 66.42, H 7.74; found C 66.73, H 8.30.

2,5-Dihydroxy-4-(3-methylbut-3-en-1-ynyl)benzaldehyde (6): To a solution of **20** (2.0 g, 4.65 mmol) in dry THF was added AcOH

(4.3 mL). After cooling to 0 °C, tetra-*n*-butylammonium fluoride (8.96 mL, 1 M in THF, 8.96 mmol) was added and the mixture stirred at 0 °C for 3 h. The mixture was then quenched with water (150 mL) and extracted with Et_2O (3×150 mL). The combined organic phases were washed with brine (100 mL), dried (MgSO_4), and the solvents evaporated in vacuo. The residue was purified by flash chromatography on silica gel (hexanes/EtOAc, 4:1) to yield **6** (0.90 g, 95.8%) as yellow crystals. M.p. 100 °C. R_f (TLC) = 0.24 (hexanes/EtOAc, 4:1). HPLC_{prep}: $R_t = 36.23$ min. UV (MeOH): λ_{max} (log ϵ) = 207 (4.27), 221 (sh, 4.24), 299 (4.23), 384 (3.91) nm. IR (KBr): $\tilde{\nu} = 3340$ (s, br), 3054 (m), 2880 (m), 2197 (w), 1804 (w), 1643 (ss), 1548 (s), 1489 (ss), 1461 (s), 1395 (m), 1344 (s), 1249 (ss), 1207 (m), 1159 (ss), 1012 (w), 896 (s), 864 (s), 804 (s), 782 (s), 657 (m), 515 (m) cm^{-1} . ^1H NMR ($[\text{D}_6]\text{DMSO}$, 300 MHz): $\delta = 1.94$ (dd, $^4J_{\text{H,H}} = 1.4, 1.1$ Hz, 3 H, 5'- CH_3), 5.39, 5.41 (each m, 1 H, 4'- CH_2), 6.88, 7.09 (each s, 1 H), 9.68, 10.10 (each s, 1 H, OH), 10.18 (s, 1 H, CHO) ppm. ^{13}C NMR ($[\text{D}_6]\text{DMSO}$, 75.5 MHz): $\delta = 23.0$ (CH_3), 84.9, 97.0 (each C_q), 112.7 (CH), 118.0 (C_q), 120.5 (CH), 122.8 (C_q), 123.2 (=CH $_2$), 126.2, 150.8 (each C_q), 150.6, 152.2, 153.0 (each C_q), 190.0 (CHO) ppm. EI-MS m/z (%) = 203 (23) [$\text{M} + \text{H}$] $^+$, 202 (100) [M^+], 201 (98) [$\text{M} - \text{H}$] $^+$, 174 (6), 173 (11), 156 (12), 117 (7), 115 (18), 91 (13). $\text{C}_{12}\text{H}_{16}\text{O}_3$ (202.06): calcd. C 71.28, H 4.98; found C 71.23, H 4.96.

Per(trimethylsilyl)ation of 6: MSTFA (10 μL) was added to 1 μg of **6** and incubated at 40 °C for 2 h to yield **23** and **24**. **23:** GC/MS: $R_t = 2045$; m/z (%) = 346 (20) [M^+], 331 (100) [$\text{M} - \text{CH}_3$] $^+$, 315 (2), 301 (1), 273 (1), 259 (1), 75 (3), 73 (9). **24:** GC/MS: $R_t = 2189$; m/z (%) = 545 (60) [M^+], 530 (21) [$\text{M} - \text{CH}_3$] $^+$, 456 (30) [$\text{M} - \text{OSi}(\text{CH}_3)_3$] $^+$, 419 (66) [$\text{M} - \text{N}(\text{CH}_3)\text{COCF}_3$] $^+$, 346 (18), 331 (100), 315 (2), 184 (4), 147 (1), 134 (7), 130 (4), 77 (13), 75 (5), 73 (25), 45 (3).

1,2,5-Trihydroxy-4-(3-methylbut-3-en-1-ynyl)benzene (7): To a solution of **6** (100 mg, 0.49 mmol) in degassed water (2 mL) and THF (5 mL) was added sodium percarbonate (80 mg, 0.50 mmol) under argon. The mixture was sonicated in an ultrasound bath for 2 h, the resulting brown solution treated with 2 N HCl (1 mL), and extracted rapidly with Et_2O (3×50 mL) (protecting gas!). The combined extracts were carefully concentrated in vacuo at 20 °C to yield **7** (80 mg, 86%) as a brownish, very unstable powder. R_f (TCL) = 0.75 (hexanes/EtOAc, 3:1). **7** was characterized by GC/MS after immediate silylation of the reaction product with MSTFA. Tris(trimethylsilyl) derivative of **7**: $R_t = 2019$, m/z (%) = 406 (48) [M^+], 391 (4), 318 (2), 303 (4), 229 (2), 147 (8), 123 (3), 97 (2), 77 (1), 75 (9), 73 (100), 59 (1), 45 (8).

2,5-Dihydroxy-4-(3-methylbutyl)benzaldehyde (22): To a solution of the aldehyde **6** (100 mg, 0.5 mmol) in dry MeOH (7 mL) was added a small portion of PtO_2 . Then, a stream of H_2 was bubbled through the solution for 1.5 h, whereby the yellow colour disappeared. Filtration of the mixture through Celite and concentration of the filtrate in vacuo gave a bright yellow solid that was purified by flash chromatography (hexanes/EtOAc, 4:1) to yield **22** (50 mg, 48%). M.p. 75 °C. R_f (TLC) = 0.32 (hexanes/EtOAc, 4:1). ^1H NMR (CDCl_3 , 300 MHz): $\delta = 0.95$ (d, $J = 6.6$ Hz, 6 H, 4'- CH_3), 1.50 (m, 2 H, 2'- CH_2), 1.62 (sept., $J = 6.6$ Hz, 1 H, 3'-CH), 2.63 (t, $J = 8$ Hz, 2 H, 1'- CH_2), 5.11 (s, 1 H, OH), 6.79, 6.90 (each s, 1 H, CH), 9.74 (s, 1 H, OH), 10.63 (s, 1 H, CHO) ppm. ^{13}C NMR (CDCl_3 , 75.5 MHz): $\delta = 22.4$ (2 CH_3), 27.9 (CH), 28.5, 38.2 (each CH_2), 117.4, 118.4 (each CH), 118.5 (C_q), 141.8, 146.8, 156.0 (each C_q), 195.3 (CHO) ppm. MS (EI): m/z (%) = 208 (81) [M^+], 153 (18), 152 (100) [$\text{M} - \text{C}_4\text{H}_8$] $^+$, 151 (63) [$\text{M} - \text{C}_4\text{H}_9$] $^+$, 124 (15), 123 (58). HRMS (EI): $m/z = 208.1104$ [M^+] (calcd. for $\text{C}_{12}\text{H}_{16}\text{O}_3$: 208.1099). $\text{C}_{12}\text{H}_{16}\text{O}_3$ (208.25): calcd. C 69.21, H 7.74; found C 69.09, H 7.72.

Per(trimethylsilyl)ation of 22: MSTFA (10 μ L) was added to 1 μ g of **22** and incubated at 40 $^{\circ}$ C for 2 h to yield **25** and **26**. **25:** GC/MS: R_f = 1965; m/z (%) = 352 (18) [M^+], 337 (100) [$M - CH_3$] $^+$, 265 (10), 75 (20), 73 (60). **26:** GC/MS: R_f = 2065; m/z (%) = 551 (40) [M^+], 536 (16) [$M - CH_3$] $^+$, 462 (25) [$M - OSi(CH_3)_3$] $^+$, 425 (100) [$M - N(CH_3)COCF_3$] $^+$, 392 (2), 353 (3), 352 (3), 351 (2), 337 (17), 279 (4), 265 (4), 184 (4), 147 (2), 134 (4), 110 (3), 77 (2), 73 (18).

Computational Methods: The conformational analyses were performed with a Linux AMD MP 2800+ workstation, in the cases of **1** and **5** by means of the semiempirical PM3^[6] method, in the case of **2** by the use of a DFT approach (B3LYP/6-31G*),^[15] as implemented in the program package Gaussian 98,^[30] starting from preoptimized geometries generated by the TRIPOS^[10] force field as part of the molecular modeling package SYBYL 7.0.^[10] The molecular dynamics simulation for **1** was performed at a virtual temperature of 500 K using the TRIPOS^[10] force field. The overall simulation time was 500 ps, the single geometries were extracted every 0.5 ps yielding 1000 conformers. The wave functions required for the computation of the rotational strengths for the electronic transitions from the ground state to excited states were obtained in the case of **1** by CNDO/S^[8] calculations followed by SCI computations including 784 singly occupied configurations and the ground-state determinant, and in the case of **5** by OM2^[17] calculations followed again by SCI computations, now including 900 singly occupied configurations as well as the ground-state determinant. These calculations were also carried out with a Linux AMD MP 2800+ workstation using the BDZDO/MCDSPD^[31] program package, and by the use of the MNDO99^[32] software package. The single CD spectra were summed up weighted according to the Boltzmann statistics, i.e., to the respective heats of formation. The rotational strengths were transformed into $\Delta\epsilon$ values and for a better visualization superimposed with a Gaussian band-shape function.

Acknowledgments

The work was supported by the Deutsche Forschungsgemeinschaft and the Fonds der Chemischen Industrie. We thank Dr. Werner Spahl for various MS experiments and Dr. Bert Steffan for extensive NMR measurements and fruitful discussions.

[1] R. Galli, *Le Russule*, Edinatura s. r. l., Milano, 1996.

[2] a) R. Aumann, H. Heinen, C. Kr ger, P. Betz, *Chem. Ber.* **1990**, *123*, 605–610; b) P. Babin, J. Dunogues, *Tetrahedron Lett.* **1983**, *24*, 3071–3074; c) K. Maruyama, A. Osuka, *J. Org. Chem.* **1980**, *45*, 1898–1901.

[3] B. Sontag, J. Dasenbrock, N. Arnold, W. Steglich, *Eur. J. Org. Chem.* **1999**, 1051–1055.

[4] a) G. Bringmann, J. M hlbacher, M. Reichert, M. Dreyer, J. Kolz, A. Speicher, *J. Am. Chem. Soc.* **2004**, *126*, 9283–9290; b) M. M ller, K. Lamottke, W. Steglich, S. Busemann, M. Reichert, G. Bringmann, P. Spittler, *Eur. J. Org. Chem.* **2004**, 4850–4855.

[5] For a discussion of empirical rules to deduce the absolute configurations of C_2 -symmetric chiral spirans, see: J. H. Brewster, R. T. Prudence, *J. Am. Chem. Soc.* **1973**, *95*, 1217–1229.

[6] J. J. P. Stewart, *J. Comput. Chem.* **1989**, *10*, 209–264.

[7] The CD spectra of those structures that lie energetically higher than 3 kcal/mol above the global minimum, do not contribute to the overall CD curve obtained by superposition of the Boltzmann-weighted single spectra.

[8] J. Del Bene, H. H. Jaff , *J. Chem. Phys.* **1968**, *48*, 1807–1813.

[9] G. Bringmann, S. Busemann, in: *Natural Product Analysis* (Eds.: P. Schreier, M. Herderich, H. U. Humpf, W. Schwab), Vieweg, Wiesbaden, **1998**, pp. 195–212.

[10] SYBYL, Tripos Associates, 1699 Hanley Road, Suite 303, St. Louis, MO 63144, USA.

[11] It should be mentioned that the minimum geometry of ochroleucin A₁ (**1**), possessing a hydrogen bond between the aldehyde oxygen atom and the *o*-phenolic hydrogen atom, was calculated to be energetically favoured over the respective minimum structure without this bonding by 7.2 kcal/mol on DFT level (B3LYP/6-31G*). In contrast, no indication of a hydrogen bond was found in the corresponding NMR experiment.

[12] W. Steglich, W. Furtner, A. Prox, *Z. Naturforsch. Teil B* **1970**, *25*, 557–558.

[13] a) E. J gers, B. Steffan, R. von Ardenne, W. Steglich, *Z. Naturforsch. Teil C* **1981**, *36*, 488–489; b) E. J gers, Dissertation, University of Bonn, **1981**.

[14] a) E. J gers, W. Steglich, *Angew. Chem.* **1981**, *93*, 1105; *Angew. Chem. Int. Ed. Engl.* **1981**, *20*, 1016–1017; b) A. M hlbauer, J. Beyer, W. Steglich, *Tetrahedron Lett.* **1998**, *39*, 5167–5170; c) A. M hlbauer, Dissertation, University of M nchen, **1998**.

[15] a) A. D. Becke, *J. Chem. Phys.* **1993**, *98*, 1372–1377; b) A. D. Becke, *J. Chem. Phys.* **1993**, *98*, 5648–5652; c) P. J. Stephens, F. J. Devlin, C. F. Chabalowski, M. J. Frisch, *J. Phys. Chem.* **1994**, *98*, 11623–11627.

[16] W. Weber, W. Thiel, *Theor. Chem. Acc.* **2000**, *103*, 495–506.

[17] A sequence **11** \rightarrow **1** \rightarrow **2** could also explain the Posternak rearrangement,^[18] in which a diquinone of type **11** is heated in a mixture of MeOH and diluted H₂SO₄. Under these reaction conditions, a spirodioxolactone of type **1** is expected to be converted into the more stable dilactone isomer **2**. Similar pathways can be suggested for the formation of dilactones from suitable benzoquinones.^[13,14,19]

[18] a) T. Posternak, W. Alcalay, R. Huguenin, *Helv. Chim. Acta* **1956**, *39*, 1556–1563; b) T. Posternak, R. Huguenin, W. Alcalay, *Helv. Chim. Acta* **1956**, *39*, 1564–1579.

[19] a) F. Kiuchi, N. Suzuki, Y. Fukumoto, Y. Goto, M. Mitsui, Y. Tsuda, *Chem. Pharm. Bull.* **1998**, *46*, 1225–1228; b) F. Kiuchi, H. Takashima, Y. Tsuda, *Chem. Pharm. Bull.* **1998**, *46*, 1229–1234.

[20] a) J.-M. Renaud, G. Tsoupras, R. Tabacchi, *Helv. Chim. Acta* **1989**, *72*, 929–932; b) P. Tey-Rulh, I. Philippe, J.-M. Renaud, G. Tsoupras, P. de Angelis, J. Fallot, R. Tabacchi, *Phytochemistry* **1991**, *30*, 471–473.

[21] K. Ishibashi, K. Nose, T. Shindo, M. Arai, H. Mishima, *San-kyo Kenkyusho Nenpo* **1968**, *20*, 76–79.

[22] A. M hlenfeld, H. Achenbach, *Phytochemistry* **1988**, *27*, 3853–3855.

[23] G. M. Dubin, A. Fkyerat, R. Tabacchi, *Phytochemistry* **2000**, *53*, 571–574.

[24] K. Orito, T. Hatakeyama, M. Takeo, H. Suginome, *Synthesis* **1995**, 1273–1277.

[25] Z. Peng, A. Gharavi, L. Yu, *J. Am. Chem. Soc.* **1997**, *119*, 4622–4632.

[26] R. C. Ronald, J. M. Lansinger, T. S. Lillie, C. J. Wheeler, *J. Org. Chem.* **1982**, *47*, 2541–2549.

[27] R. K. Crowden, *Can. J. Microbiol.* **1967**, *13*, 181–197.

[28] G. Vidari, P. Vita-Finzi, A. M. Zanolchi, *J. Nat. Prod.* **1995**, *58*, 893–896.

[29] M. De Bernardi, G. Vidari, P. Vita-Finzi, G. Fronza, *Tetrahedron* **1992**, *48*, 7331–7344.

[30] M. J. Frisch, G. W. Trucks, H. B. Schlegel, G. E. Scuseria, M. A. Robb, J. R. Cheeseman, V. G. Zakrzewski, J. A. Montgomery, Jr., R. E. Stratmann, J. C. Burant, S. Dapprich, J. M. Millam, A. D. Daniels, K. N. Kudin, M. C. Strain, O. Farkas, J. Tomasi, V. Barone, M. Cossi, R. Cammi, B. Mennucci, C. Pomelli, C. Adamo, S. Clifford, J. Ochterski, G. A. Petersson, P. Y. Ayala, Q. Cui, K. Morokuma, D. K. Malick, A. D. Rabuck, K. Raghavachari, J. B. Foresman, J. Cioslowski, J. V. Ortiz, A. G. Baboul, B. B. Stefanov, G. Liu, A. Liashenko, P. Piskorz, I. Komaromi, R. Gomperts, R. L. Martin, D. J. Fox, T. Keith, M. A. Al-Laham, C. Y. Peng, A. Nanayakkara, C. Gonzalez, M. Challacombe, P. M. W. Gill, B. Johnson, W. Chen,

- M. W. Wong, J. L. Andres, C. Gonzalez, M. Head-Gordon, E. S. Replogle, J. A. Pople, *Gaussian 98*, revision A.7, Gaussian, Inc., Pittsburgh, PA, USA, **1998**.
- [31] J. W. Downing, *Program Package BDZDO/MCDSPD*, Department of Chemistry and Biochemistry, University of Colorado, Boulder, CO, USA; modified by J. Fleischhauer, W. Schleker, B. Kramer; ported to Linux by K.-P. Gulden.
- [32] W. Thiel, *Software Package MNDO99*, version 6.0, Max-Planck-Institut für Kohlenforschung, Kaiser-Wilhelm-Platz 1, 45470 Mülheim, Germany.

Received: September 20, 2005
Published Online: December 12, 2005